The 2013 World Congress on
Advances in Structural Engineering and Mechanics (ASEM13)
Jeju, Korea, September 8-12, 2013

Seismic fragility curve development by coupling FERUM and ZEUS-NL

*Young-Joo Lee[1] and Do-Soo Moon[2]

[1] *School of Urban and Environmental Eng., UNIST, Ulsan 689-798, Korea*
[2] *Department of Civil and Environmental Eng., Univ. of Illinois, Urbana, IL 61801, USA*
[1] *ylee@unist.ac.kr*

ABSTRACT

Accurate seismic fragility curve has been recognized as a key to effective seismic risk assessment and management. Existing methodologies for seismic fragility curve development can be classified into four groups: empirical, judgmental, analytical, and hybrid. Among them, analytical fragility curves are most widely used, and they can be categorized again into two subgroups, depending on whether one is using an analytical function or a simulation technique. Although the both types have shown decent performances in many seismic fragility problems, they often over-simplify the given problems in reliability analysis or structural analysis due to their own assumptions. In this paper, a new methodology for seismic fragility curve development is proposed. By coupling sophisticated software packages of reliability analysis (FERUM) and structural analysis (ZEUS-NL), the methodology enables us to obtain more accurate seismic fragility curves for less computational cost. In addition, it provides not only component probabilities, but also useful byproducts that allow us to perform the fragility analysis at system level. The proposed methodology is applied to a numerical example of a 2D frame structure and the results are compared with those by Monte Carlo simulation, demonstrating that the method derives seismic fragility curves accurately and efficiently.

1. INTRODUCTION

There have been continuous efforts to estimate earthquake losses and manage the risk through seismic risk assessment. To the efforts, accurate seismic fragility curve has been recognized as a key. For example, HAZUS (NIBS 1999) and MAEviz (Elnashai *et al*. 2008) employ seismic fragility curves to predict various post-earthquake losses given certain scenario earthquake. Such predictions provide the users with a basis for decision-making on structural management, and help them reduce seismic losses (Kircher *et al*. 2006). Therefore, the development of accurate seismic fragility curves is essential for effective seismic risk assessment and management.

---

[1] Assistant Professor
[2] Postdoctoral Research Associate

A seismic fragility curve shows the relationship between ground shaking intensity (for example, peak ground acceleration or spectral acceleration) and the likelihood that a structure reaches at least certain response level (Jeong and Elnashai 2007). In other words, a seismic fragility curve displays the susceptibility of a structure to damage caused by ground shaking of given intensity.

There have been many methodologies developed for deriving seismic fragility curves. According to Rossetto and Elnashai (2003), existing types of fragility curve can be categorized into four groups: empirical, judgmental, analytical, and hybrid, depending on whether the damage data used for their derivation are acquired from the post-earthquake surveys, expert opinion, analytical simulation, or combinations of these. Although empirical and judgmental fragility curves may be more realistic than the others because they are derived from observed damage or expert opinion regarding actual structures, they have limitations in their general application (Kwon 2007).

For this reason, analytical methodologies are widely used for the development of seismic fragility curves, and they are classified again into two subgroups depending on whether the methodologies are using an analytical function or a simulation technique (Rossetto and Elnashai 2003). First, in analytical-function-based methodologies, the structural behavior or the probability of a structure will exceed a certain response level is expressed as an analytical function of related parameters such as peak ground acceleration (PGA), peak ground velocity (PGV), structural natural period, and the response threshold of interest. Based on such analytical functions, the seismic fragility curves are derived analytically. During the analytical derivation, however, the structural behavior and exceedance probability are commonly over-simplified. For example, only single-degree-of-freedom (SDOF) analysis or static analysis is allowed, rather than nonlinear response history analysis, due to the assumptions of the approach (Kwon 2007). Reliability and structural analyses are often considered as the two cores of seismic fragility analysis, and in the analytical-function-based methodologies, the former may be performed rigorously but the latter may not.

On the other hand, in the simulation-based methodologies, seismic fragility curves can be obtained through rigorous structural analysis. These methodologies generally require generating a certain number of random variable sets, performing sophisticated structural analysis for each one, and checking if the corresponding structural response exceeds certain level or not. This type of approach is straightforward to implement and very useful for a complex seismic risk problem with several random variables and structural failure modes. Speaking of the two cores of seismic fragility analysis in these simulation-based approaches, structural analysis is done rigorously because sophisticated structural analysis (e.g., pushover analysis and dynamic response-history analysis) can be introduced, and simulation methods (e.g., Monte Carlo simulation (MCS)) also have obtained a good reputation for accuracy from the reliability analysis communities.

However, there is a considerable disadvantage when using simulation-based methodologies for seismic fragility curve development: they often require a large number of structural analyses for reliable outcomes, and the simulation number increases when the level of expected probability outcome is low. This is not a serious issue if each structural analysis can be done very quickly. However, the efficiency of

the fragility analysis may suffer when sophisticated and expensive structural analysis needs to be introduced.

To overcome these disadvantages of the existing analytical methodologies, this paper presents a new analytical methodology for seismic fragility curve development. Basically, it relies on an analytical reliability analysis method instead of any simulation-based technique, so it can expect better efficiency. In order to perform seismic fragility analysis employing an analytical method of reliability analysis, an interface code between reliability analysis and structural analysis software packages is developed. By coupling the two packages, it is possible to derive more accurate seismic fragility curves for less computational cost.

2. RELIABILITY ANALYSIS METHODS

A number of reliability analysis methods have been developed and adopted in various engineering disciplines (Haldar 2006). They can be classified into two groups, sampling-based methods and analytical (or non-sampling-based) methods, which can be represented by Monte Carlo simulation (MCS) and first order reliability method (FORM), respectively. The detailed review of the two methods can be found in Melchers (1999) and Der Kiureghian (2005). In this paper, FORM is employed to overcome the disadvantages of using MCS for the derivation of seismic fragility curves, and the methods are briefly explained in this section for a comparison purpose.

2.1 First Order Reliability Method (FORM)

Let us consider a limit-state function to express an event of interest. In a structural reliability problem, the limit-state function is termed by $g(\mathbf{x})$ and the event of interest (often called "failure") is expressed by $g(\mathbf{x}) \leq 0$ where $\mathbf{x}$ is a column vector of n random variables (i.e. $\mathbf{x}=[x_1, x_2,..., x_n]^T$) representing the uncertainties in the given problem. Then the probability of the event P_f is

$$P_f = P[g(\mathbf{x}) \leq 0] = \int_{g(\mathbf{x})\leq 0} f_{\mathbf{x}}(\mathbf{x}) d\mathbf{x} \tag{1}$$

where $f_{\mathbf{x}}(\mathbf{x})$ is the joint probability density function (PDF) of $\mathbf{x}$. Transforming the space of random variables into the standard normal space, the probability P_f can be expressed as

$$P_f = \int_{g(\mathbf{x})\leq 0} f_{\mathbf{x}}(\mathbf{x}) d\mathbf{x} \int_{G(\mathbf{u})\leq 0} \varphi_n(\mathbf{u}) d\mathbf{u} \tag{2}$$

where $G(\mathbf{u})=g(\mathbf{T}^{-1}(\mathbf{u}))$ is the transformed limit-state function in the standard normal space, $\varphi_n(\cdot)$ denotes the n-th order standard normal PDF, $\mathbf{u}$ is the column vector of n standard normal variables, and $\mathbf{T}$ is the one-to-one mapping transformation matrix satisfying $\mathbf{u}=\mathbf{T}(\mathbf{x})$.

In the first order reliability method (FORM), the probability (i.e. P_f in Eq. (2)) can be approximated by linearizing the function $G(\mathbf{u})$ at a point $\mathbf{u}^*$ which is defined by the following constrained optimization problem:

$$\mathbf{u}^* = \arg\min\left\{\|\mathbf{u}\| \,\middle|\, G(\mathbf{u}) = 0\right\} \tag{3}$$

where —argmin" denotes the argument of the minimum of a function and ||·|| is the L^2-norm. In Eq. (3), it is seen that $\mathbf{u}^*$ is located on the limit-state surface satisfying $G(\mathbf{u})=0$, and has the minimum distance from the origin in the standard normal space. As an example of the first-order approximation concept of FORM, Fig. 1 shows the approximated limit-state function in the two-dimensional space.

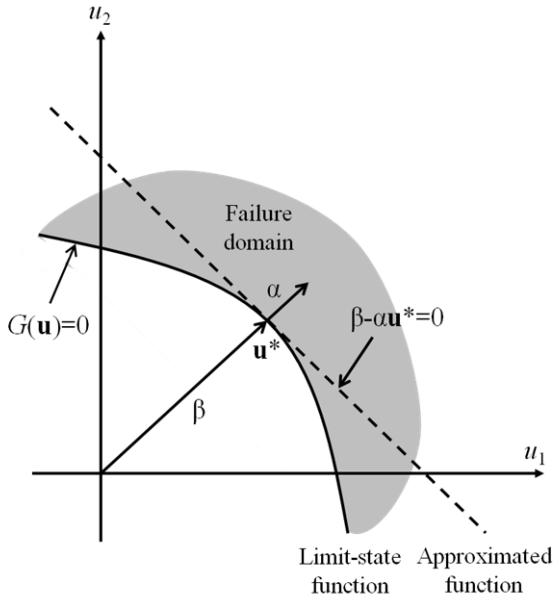

Fig. 1 Linear approximation in FORM

In the standard normal space shown in the figure, since equal probability density contours are concentric circles centered at the origin, $\mathbf{u}^*$ has the highest probability among all of the nodes in the failure domain, $G(\mathbf{u})\leq 0$. In this sense, $\mathbf{u}^*$ is an optimal point and commonly called *design point* or *most probable point* (MPP).

Noting that $G(\mathbf{u}^*)=0$, the limit-state function approximated at MPP is written as

$$G(\mathbf{u}) \cong \nabla G(\mathbf{u}^*)(\mathbf{u}-\mathbf{u}^*) = \|\nabla G(\mathbf{u}^*)\|(\beta - \alpha\mathbf{u}) \tag{4}$$

where $\nabla G(\mathbf{u})=[\partial G/\partial u_1,\ldots, \partial G/\partial u_n]$ denotes the gradient vector, $\boldsymbol{\alpha}=-\nabla G(\mathbf{u}^*)/\|\nabla G(\mathbf{u}^*)\|$ is the normalized negative gradient vector at MPP (i.e. a unit vector normal to the limit-state surface at MPP), and $\beta=-\boldsymbol{\alpha}\mathbf{u}^*$ is the reliability index.

One of the representative methods to solve the constrained optimization problem in Eq. (3) is the HL-RF algorithm summarized in Fig. 2. The details of the algorithm and FORM can be found in Rackwitz and Fiessler (1978) and in Der Kiureghian (2005). In

the following numerical example, ε_1, ε_2, and i_{max} are assumed to be 0.05, 0.05, and 20, respectively.

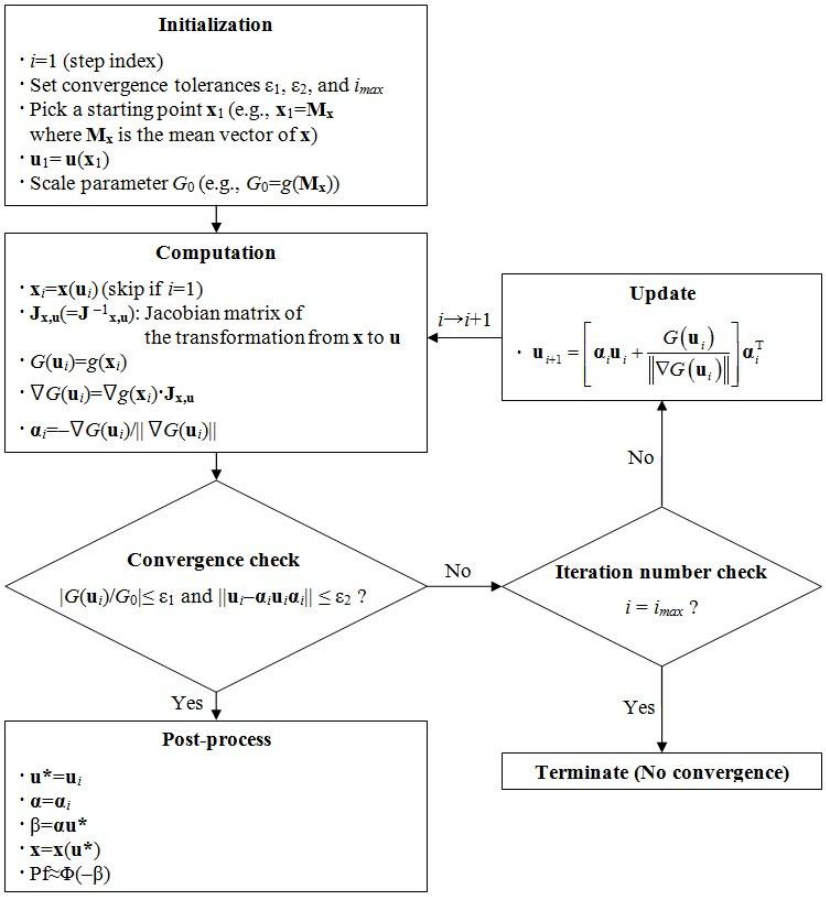

Fig. 2 FORM by HL-RF algorithm (Song 2007)

2.2 Monte Carlo Simulation (MCS)

Compared with FORM, MCS is conceptually straightforward. To estimate the failure probability in a structural reliability problem, it needs to generate n_S sample sets of random variables. Each random variable set is used to run structural analysis and to check whether the given structure is turned out to fail or not. Then the failure probability P_f is

$$P_f = n_f / n_s \tag{5}$$

where n_f is the number of sample sets which satisfy $g(\mathbf{x})\leq 0$. Unlike the result from FORM, the one from MCS is not a closed form solution and always has sampling error. The MCS result converges to a closed form solution as the number of samples increases, but the error cannot be completely eliminated unless the number of samples is infinite.

Furthermore, MCS can be computationally very expensive and the convergence of failure probability result may be slow, depending on the cost of structural analysis.

According to Haldar and Mahadevan (2000), the minimum number of samples (N_δ) to achieve a target level of c.o.v.(δ), coefficient of variation, is calculated by

$$N_\delta = \frac{1-P_f}{\delta^2 P_f} \tag{6}$$

where P_f is the failure probability from MCS.

Fig. 3 shows, in semi-log scale, the relationship between the minimum number of samples (N_δ) and failure probability (P_f) for several c.o.v. (δ) values. To achieve 5% c.o.v. which is often accepted by researchers as a reasonable level, for example, it is required using about 3.6×10^3, 7.6×10^3, and 3.96×10^4 samples and performing the same numbers of structural analyses when the expected failure probabilities are respectively 0.1, 0.05, and 0.01. Furthermore, the computational cost will significantly increase if a lower level of probability is expected or one aims to achieve a high level of convergence (i.e. low c.o.v. value) in failure probability calculation. However, it is impractical to perform such a huge number of structural analyses even though each analysis takes only a few minutes. Especially, in the case that each structural analysis is expensive (such as with nonlinear inelastic response history analysis), it would be almost impossible to achieve a reliable level of failure probability using MCS.

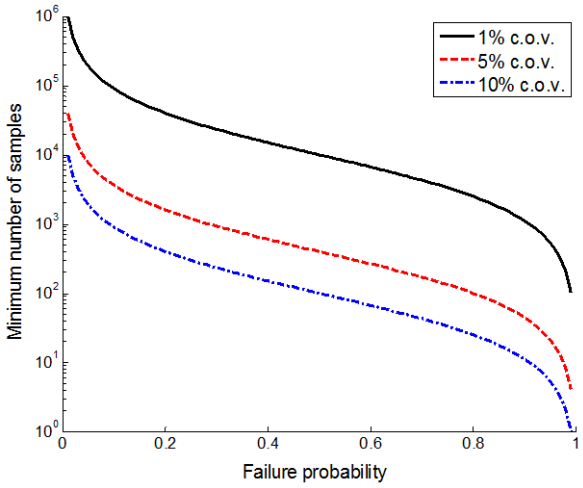

Fig. 3 The minimum number of samples with varying failure probability and c.o.v.

3. SEISMIC FRAGILITY ANALYSIS PLATFORM INTEGRATED WITH FERUM AND ZEUS-NL

To overcome the shortcomings of MCS and introduce FORM into fragility curve development, in this paper, two software packages of reliability and structural analyses are coupled. According to Haukaas (2003), the first attempt to couple reliability analysis algorithms and structural analysis methods was made by Der Kiureghian and Taylor (1983). Since then, there have been many studies leading to develop various software packages for structural reliability analysis. These developed software packages can be

categorized into two groups depending on how the structural analysis module is integrated with the reliability analysis module. In the programs of the first group, such as CalREL (Liu *et al*. 1989) and FERUM (Haukaas 2003), the probabilistic model is expressed by algebraic functions or user-defined algorithms involving basic random variables. These software packages have their own structural analysis modules or require users to analytically express the limit state of their interests in terms of random variables. For this reason, many programs in this group are limited to linear structural models.

On the contrary, those in the second group, such as NESSUS (SwRI 2009) and STRUREL (Gollwitzer *et al*. 2006), allows their users to introduce sophisticated structural analysis methods (e.g., finite element methods) to represent the structural behavior accurately. As an extended effort in this trend, an interface code between FERUM and ABAQUS® (termed the FERUM-ABAQUS) was developed. By coupling the two software packages specialized in their own areas, it becomes possible to take full advantages of them and solve challenging structural reliability problems about aircraft wing torque box (Lee *et al*. 2008) and cable-stayed bridge pylon (Kang *et al*. 2012).

However, such coupling techniques have not been applied to develop seismic fragility curves. In order to perform seismic fragility analysis based on the proposed methodology, two external software packages which respectively execute reliability analysis and structural analysis need to be coupled. In this paper, FERUM and ZEUS-NL are selected, and an interface code has been developed so that these two software packages can communicate with each other during fragility analysis. The computational platform integrated with FERUM and ZEUS-NL is called FERUM-ZEUS hereafter. By coupling reliability analysis software (FERUM) and structural analysis software (ZEUS-NL), the new methodology allows us to obtain more accurate seismic fragility curves for less computational cost.

FERUM (Finite Element Reliability Using Matlab) is a reliability analysis package developed by researchers at the University of California at Berkeley, which allows us to perform various reliability analyses (Haukaas 2003). FERUM offers functions from various reliability analysis methods including FORM, SORM (Second order reliability method), MCS, and importance sampling simulation, and most of the common probability distribution types are available for the program. In addition, the program opens its source codes to public (www.ce.berkeley.edu/FERUM). Because of these attractive features, FERUM has been widely applied to various engineering problems.

ZEUS-NL (Elnashai *et al*. 2010) is a fiber-element-based nonlinear analysis program developed by Mid-America Earthquake (MAE) Center. It is one of the advanced structure analysis packages, specifically for earthquake engineering applications. ZEUS-NL can represent spread of inelasticity within the member cross-section as well as along the member length utilizing the fiber analysis approach. Also, this program opens its source codes to public (http://code.google.com/p/zeus-nl/).

Fig. 4 shows the data flow of in FERUM-ZEUS. For the numerical example in this paper, we use the first order reliability method (FORM) available in the open-source reliability code FERUM. In order to solve the nonlinear constrained optimization problem in Eq. (3) using FORM, as addressed in Fig. 2, $G(\mathbf{u}_i)$ and $\nabla G(\mathbf{u}_i)$ (i.e. the values and gradients of the limit-state function in the standard normal space) are

required at each step of the iteration. If the limit-state function is expressed by random variables **x**, it is also possible to obtain the gradient values analytically (i.e. by $\nabla G(\mathbf{u}_i) = \nabla g(\mathbf{u}_i) \cdot \mathbf{J}_{\mathbf{x},\mathbf{u}}$). However, if the limit-state function is not an analytical function of random variable, it is a challenging task to calculate the gradients during the FORM analysis. The interface module between FERUM and ZEUS-NL is developed such that FERUM can obtain the limit-state function values from the output responses, e.g., force or displacement results evaluated by a structural analysis performed by ZEUS-NL, and the gradients are achieved numerically, by using finite difference method. For this reason, the number of limit-state function evaluations n_{fe} during the FORM analysis is

$$n_{fe} = (n_{RV} + 1) \times n_i \tag{7}$$

where n_{RV} and n_i denote the number of random variables (RVs) and the number of iterations.

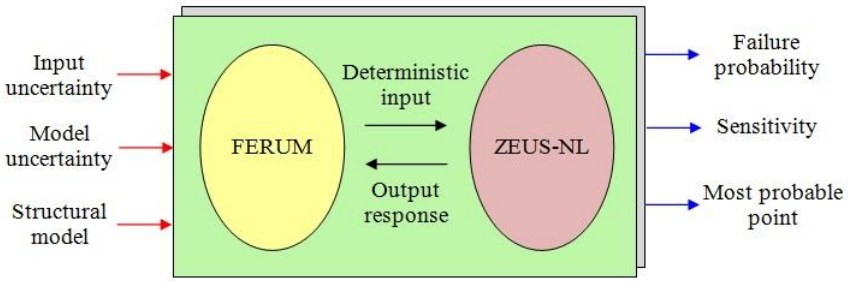

Fig. 4 Data flow in FERUM-ZEUS

In the proposed platform, the reliability analysis package FERUM repeatedly calls ZEUS-NL to obtain structural responses during component reliability analysis employing FORM. By employing ZEUS-NL which is specialized in nonlinear response history analysis, FERUM can perform reliability analysis accurately based on sophisticated structural analysis.

4. NUMERICAL EXAMPLE: 2D FRAME BUILDING

In order to verify the proposed method and to highlight its advantages, a benchmark problem is chosen and solved. Kwon and Elnashai (2006) performed fragility analyses with 2D frame buildings to develop their fragility curves and to investigate the effect of material and ground motion uncertainty on them. A three-story reinforced concrete frame was utilized for their study, and seismic fragility curves of the given structure were derived through MCS with nine sets of input ground motions. In this paper, the same structure is investigated as a benchmark model. The proposed method employing FERUM-ZEUS is applied to derive the fragility curves, and they are compared with those from MCS in the study of Kwon and Elnashai (2006).

4.1 Problem Description

4.1.1 Structural configuration

The three-story reinforced concrete moment frame, presented in the study of Kwon and Elnashai (2006), is utilized as a prototype structure. As shown in Fig. 5, it has three bays in the longitudinal direction and the length of a bay is 5.49 m (18 ft). The height of each story is 3.66 m (12 ft) and the total height is 10.98 m (36 ft). The analytical model is created in the nonlinear finite element analysis (FEA) program, ZEUS-NL, as depicted in Fig. 6. Columns and beams are divided into six and seven elements, respectively. The twelve columns are referred as to C01-C04 (on the 1st story), C11-C14 (on the 2nd story), and C21-C24 (on the 3rd story). Lumped masses are placed at the beam-column connections. In the model, only hysteretic damping is considered by nonlinear material modeling. For detailed information, reference is made to Bracci *et al*. (1992) and Kwon and Elnashai (2006).

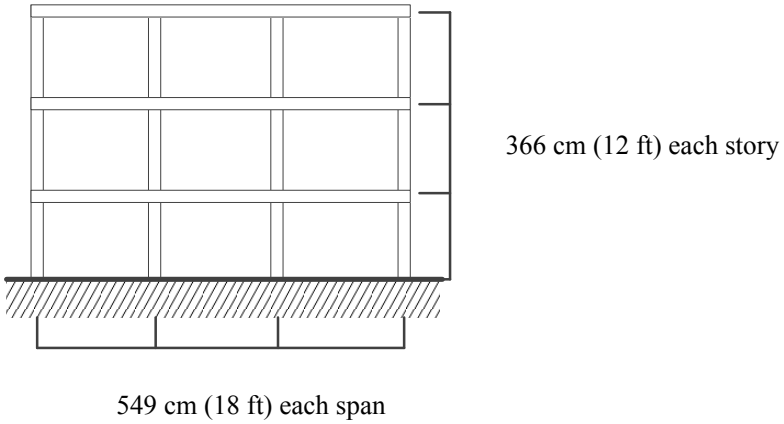

Fig. 5 Plan (left) and elevation (right) views of prototype structure

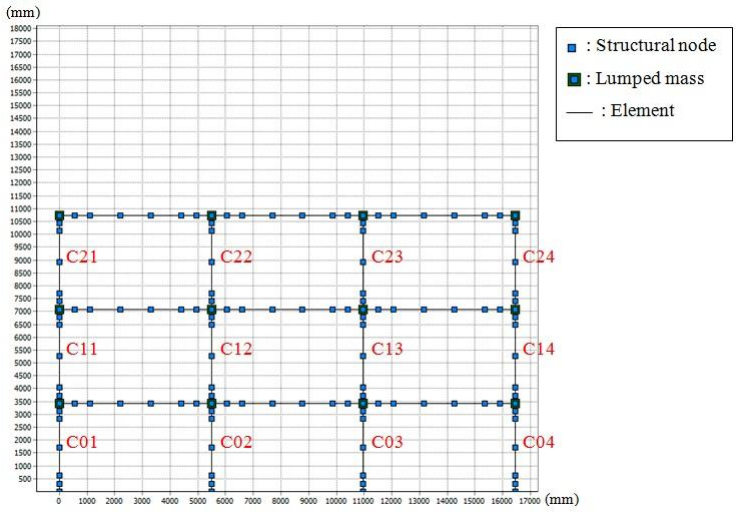

Fig. 6 Structural model constructed for FERUM-ZEUS

4.1.2 Input ground motions

In the research of Kwon and Elnashai (2006), nine ground motion sets were used for the derivation of fragility curves. The first three sets are based on the ratio of peak ground acceleration to peak ground velocity (*a*/*v*), and the other six are artificial ground motions generated with different soil profiles in the Memphis area. Among those nine sets, this study employs the first three ground motions sets, which are based on *a*/*v* ratio. These sets have low, intermediate and high *a*/*v* respectively, and each set has five input ground motions selected based on the following categorization.

$$\begin{aligned} &\text{Low}: a/v < 0.8g/\text{m}\cdot\text{s}^{-1} \\ &\text{Intermediate}: 0.8g/\text{m}\cdot\text{s}^{-1} \le a/v \le 1.2g/\text{m}\cdot\text{s}^{-1} \\ &\text{High}: 1.2g/\text{m}\cdot\text{s}^{-1} < a/v \end{aligned} \tag{8}$$

Table 1 summarizes the properties of the selected ground motions, and Figs. 7-9 show acceleration time histories of them.

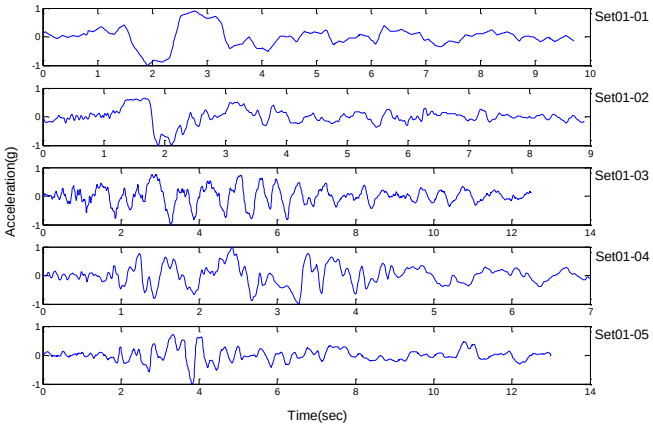

Fig. 7 Input ground motions with low a/v ratio

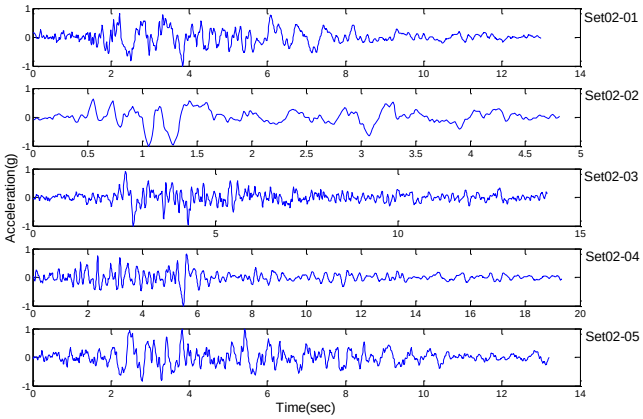

Fig. 8 Input ground motions with intermediate a/v ratio

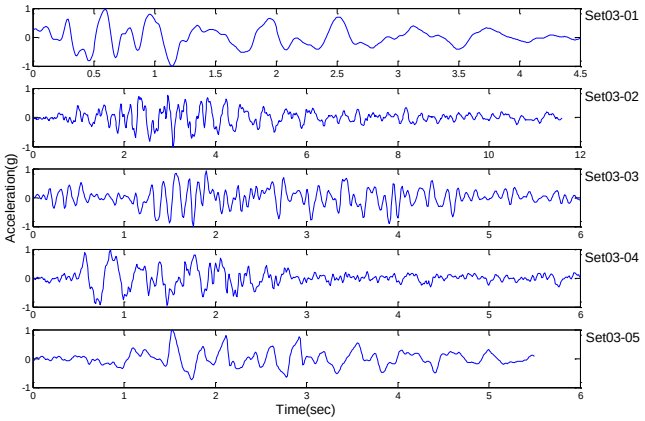

Fig. 9 Input ground motions with high a/v ratio

Table 1 Properties and names of input ground motions, after: (Kwon and Elnashai 1980)

a/*v* ratio	Name	Earthquake event/Location	Magnitude	Date	Soil type	Distance (km)	Maximum acceleration (m/s^2)	*a*/*v* ratio (g/ms^{-1})
Low	Set01-01	Bucharest/Romania	6.40	3/4/1977	Rock	4	−1.906	0.275
	Set01-02	Erzincan/Turkey	Unknown	3/13/1992	Stiff soil	13	−3.816	0.382
	Set01-03	Aftershock of Montenegro/Yugoslavia	6.20	5/24/1979	Alluvium	8	−1.173	0.634
	Set01-04	Kalamata/Greece	5.50	9/13/1986	Stiff soil	9	−2.109	0.657
	Set01-05	Kocaeli/Turkey	Unknown	8/17/1999	Unknown	101	−3.039	0.750
Inter-mediate	Set02-01	Aftershock of Friuli/Italy	6.10	9/15/1976	Soft soil	12	−0.811	1.040
	Set02-02	Athens/Greece	Unknown	9/7/1999	Unknown	24	−1.088	1.090
	Set02-03	Umbro-Marchigiano/Italy	5.80	9/26/1997	Stiff soil	27	−0.992	1.108
	Set02-04	Lazio Abruzzo/Italy	5.70	5/7/1984	Rock	31	−0.628	1.136
	Set02-05	Basso Tirreno/Italy	5.60	4/15/1978	Soft soil	18	0.719	1.183
High	Set03-01	Gulf of Corinth/Greece	4.70	11/4/1993	Stiff soil	10	−0.673	1.432
	Set03-02	Aftershock of Montenegro/Yugoslavia	6.20	5/24/1979	Rock	32	−0.667	1.526
	Set03-03	Aftershock of Montenegro/Yugoslavia	6.20	5/24/1979	Alluvium	16	−1.709	1.564
	Set03-04	Aftershock of Umbro-Marchigiana/Italy	5.00	11/9/1997	Rock	2	0.412	1.902
	Set03-05	Friuli/Italy	6.30	5/6/1976	Rock	27	3.500	1.730

4.1.3 Statistical parameters

Three kinds of uncertainties, which are in input ground motion, concrete strength, and steel strength, are considered, as presented in the study of Kwon and Elnashai (2006). The first one characterizes the uncertainty in loads or demand, and the other two represent the uncertainties in the material properties or supply. Uncertainty in the demand is accounted for by using sets of ground motions while uncertainties in the supply are represented by two random variables: concrete and steel strength. Table 2 summarizes the mean, coefficient of variation (c.o.v.), and the type of distribution used for those random variables. These statistical properties are the same as those in the study of Kwon and Elnashai (2006).

Table 2 Statistical properties of random variables

Random variables (RVs)	Mean (MPa)	c.o.v.	Distribution type	Number of RVs
Concrete strength (f_c)	33.6	0.186	Normal	1
Steel strength (f_y)	336.5	0.107	Normal	1

4.1.4 Limit states

As defined in the study of Kwon and Elnashai (2006), three limit states of *serviceability*, *damage control* and *collapse prevention* are employed, and they correspond to inter-story drift of 0.57%, 1.2%, and 2.3%, respectively. There are a total of twelve columns (i.e., four columns on each of three stories) in the prototype structure, and it is assumed that a limit state is achieved if its inter-story drift criterion is met at any column. With this assumption, limit-state functions can be defined as follows:

$$\text{Serviceability:} \quad g(\mathbf{x}) = 0.0057 - \max\left[ISD_{C01}(\mathbf{x}), ISD_{C02}(\mathbf{x}), ..., ISD_{C24}(\mathbf{x})\right] \le 0 \tag{9a}$$

$$\text{Damage control:} \quad g(\mathbf{x}) = 0.012 - \max\left[ISD_{C01}(\mathbf{x}), ISD_{C02}(\mathbf{x}), ..., ISD_{C24}(\mathbf{x})\right] \le 0 \tag{9b}$$

$$\text{Collapse prevention:} \quad g(\mathbf{x}) = 0.023 - \max\left[ISD_{C01}(\mathbf{x}), ISD_{C02}(\mathbf{x}), ..., ISD_{C24}(\mathbf{x})\right] \le 0 \tag{9c}$$

where ISDC01, ISD C02,…, ISDC24 denote the inter-story drift (ISD) ratios of the twelve columns (C01-C04, C11-C14, and C21-C24) in Fig. 6.

4.2 Analysis Results

Fig. 10 shows fragility curves from the proposed method for the three limit states. There are significant differences in the fragility curves from different ground motion sets, but the overall trend is that the exceedance probability increases with the decreasing IDS threshold as well as with the increasing PGA.

The fragility curve results in the figure are fairly similar to those in the study of Kwon and Elnashai (2006), especially in the range of high exceedance probability. However, it is stated by Kwon and Elnashai (2006) that they performed a total of 23,000 response history analyses, which means 100 simulations (i.e. 100 structural analyses) for each input ground motion at each PGA. This is the reason that some differences in the fragility values are observed between those from the proposed method and those of Kwon and Elnashai (2006). In order to confirm the sources of the differences, MCS with up to 1,000 samples are conducted for three selected cases, Case1, Case2, and Case3. The results are summarized in Table 3. The proposed method calculates the probabilities of the three cases to be 2.32×10^{-2}, 1.00×10^{-1}, and 6.22×10^{-1} for only 21, 18, and 12 structural analyses respectively.

Table 3 Three selected cases

Case name	Input ground motion	PGA (g)	Limit State	Probability from the propose method	Number of structural analyses
Case1	Set02-01	0.08	Serviceability	2.32×10^{-2}	21
Case2	Set03-04	0.35	Damage control	1.00×10^{-1}	18
Case3	Set01-05	0.25	Collapse prevention	6.22×10^{-1}	12

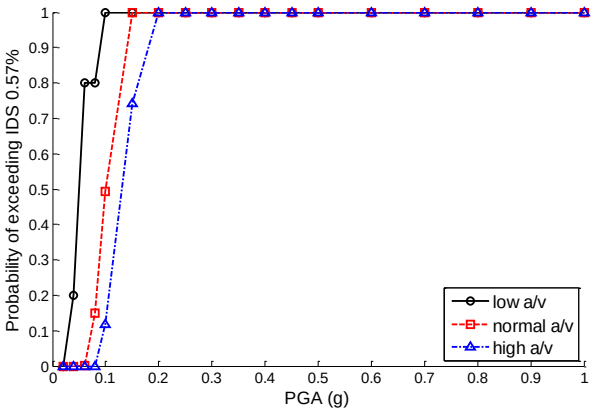

(a) Serviceability limit-state

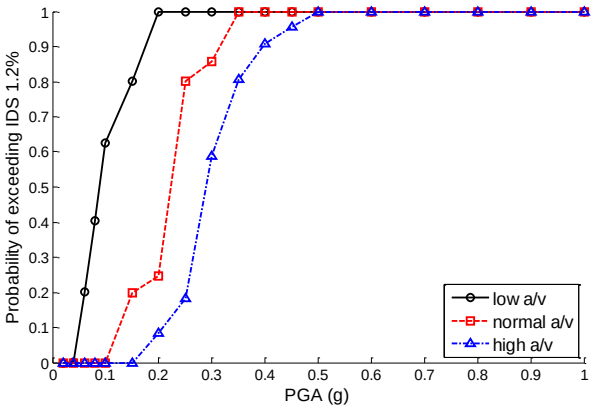

(b) Damage control limit-state

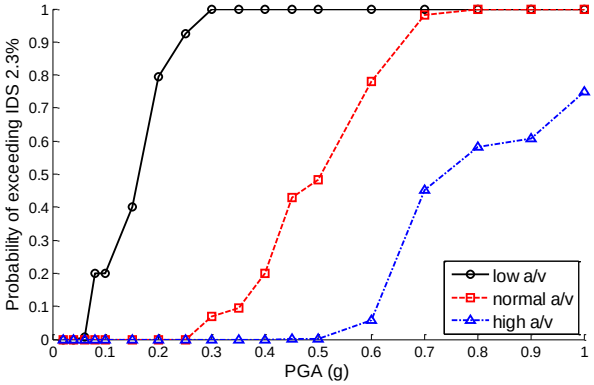

(c) Collapse prevention limit-state

Fig. 10 Fragility curves for three limit states

Fig. 11 shows how the probabilities from MCS for the three cases converge as the number of samples increases. Although the probability converges very quickly in Case3 because the expected probability level (i.e. 6.22×10^{-1}, shown with the blue dotted line) is relatively high, the probability convergence is not achieved even with 1,000 samples in Case1 because the expected probability level (i.e. 2.32×10^{-2}, shown with the blue dotted line) is very small.

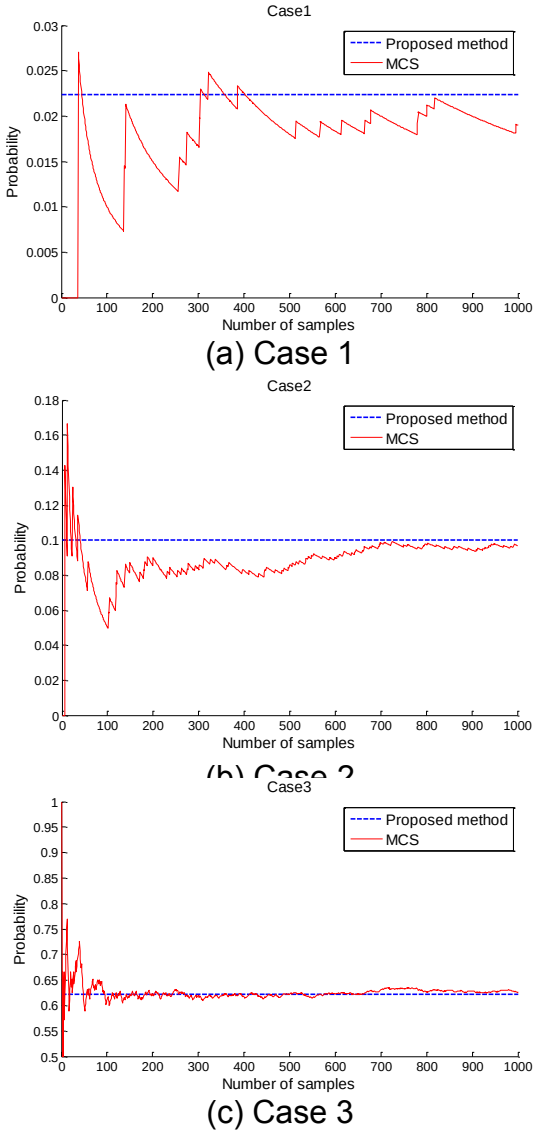

Fig. 11 Probabilities from MCS with the increasing number of samples for the three cases

Overall, the number of limit-state function evaluations (or structural analyses) required for the FORM analysis in the proposed method is small. The required number of limit-state function evaluations n_{fe} can be calculated by use of Eq. (7). In the numerical example, the maximum cost of the structural analyses by the proposed method is 60 because there are 2 random variables and a maximum of 20 iterations. The cost can be reduced when convergence is achieved during the FORM analysis, as shown in Table 3.

However, it should also be noted that the computational efficiency of the proposed method may suffer if there are a large number of random variables in a problem. As shown in Eq. (7), the required number of limit-state function evaluations n_{fe} is proportional to (n_{RV} +1). For this reason, it may be better to use one of the advanced simulation-based methods when many random variables need to be assumed. In many

structural problems, however, several random variables are enough to represent the uncertainties in the structure, and the proposed method can be useful for such cases.

Another noticeable aspect of the proposed method is, since convergence may not be achieved during the FORM analysis depending on the shape of the limit-state surface, the proposed methodology employing FORM may not work properly if the failure domain of interest is very complex. In such a case, another methodology introducing advance simulation-based/non-simulation-based techniques may be preferable.

5. SUMMARY AND CONCLUSIONS

In this paper, a new methodology for the development of seismic fragility curves is proposed. By being integrated with sophisticated software packages of reliability analysis and structural analysis, the new method can generate more accurate seismic fragility curves for less computational cost than simulation-based methods. Accordingly, as a computational platform of the proposed method, FERUM-ZEUS is newly developed. In this platform, the reliability analysis package FERUM repeatedly calls ZEUS-NL to obtain structural responses of interest during component reliability analysis. Since the proposed method performs reliability analysis using the first order reliability method (FORM), it provides component probabilities. The new methodology is applied to the numerical example of a 2D frame building. The comparison of the results with those found by Monte Carlo simulation indicates that the method generates seismic fragility curves accurately and efficiently. Through the numerical example, it is proved that, by using proposed methodology, accurate seismic fragility curves can be obtained at a moderate computational cost.

REFERENCES

Bracci, J.M., Reinhorn, A.M. and Mander, J.B. (1992), Seismic Resistance of Reinforced Concrete Frame Structures Designed Only for Gravity Loads: Part I—Design and Properties of a One-third Scale Model Structure, Technical report, National Center for Earthquake Engineering Research, Buffalo, NY, USA.

Der Kiureghian, A. (2005), —First- and Second-order Reliability Methods", Engineering Design Reliability Handbook, (edited by Nikolaidis, E., Ghiocel, D.M. and Singhal, S.), CRC Press, Boca Raton, FL, USA, Chap. 14.

Der Kiureghian, A. and Taylor, R. L. (1983), —Numerical methods in structural reliability", 4th International Conference on Applications of Statistics and Probability in Civil Engineering (ICASP4), Florence, Italy, June.

Elnashai, A., Hampton, S., Karaman, H., Lee, J.S., McLaren, T., Myers, J., Navarro, C., Sahin, M., Spencer, B. and Tolbert, N. (2008), —Overview and applications of MAEviz – HAZTURK 2007", J. of Earthq. Eng., 12(1), 100-108.

Elnashai, A.S., Papanikolaou, V.K. and Lee, D. (2010), ZEUS NL - A System for Inelastic Analysis of Structures, User's manual, Mid-America Earthquake (MAE) Center, Department of Civil and Environmental Engineering, University of Illinois at Urbana-Champaign, Urbana, IL, USA.

Gollwitzer, S., Kirchgaßner, B., Fischer, R. and Rackwitz, R. (2006), —PERMAS-RA/STRUREL system of programs for probabilistic reliability analysis", Struct. Saf., 28, 108–129.

Haldar, A. (2006), Recent Developments in Reliability-based Civil Engineering, World Scientific Publishing Company, Singapore.

Haldar, A. and Mahadevan, S. (2000), Probability, Reliability, and Statistical Methods in Engineering Design, John Wiley & Sons, New York, NY, USA.
Haukaas, T. (2003), "Finite element reliability and sensitivity methods for performance-based engineering", Ph.D. Dissertation, University of California, Berkeley, CA, USA.
Jeong, S. and Elnashai, A.S. (2007), "Probabilistic fragility analysis parameterized by fundamental response quantities", Eng. Struct., 29, 1238–1251.
Kang, W.-H., Lee, Y.-J., Song, J. and Gencturk, B. (2012), "Further development of matrix-based system reliability method and applications to structural systems", Struct. and Infrastruct. Eng., 8(5), 441-457.
Kircher, C.A., Whitman, R.V. and Holmes, W.T. (2006), "HAZUS Earthquake Loss Estimation Methods", Nat. Hazards Rev., 7(2), 45-59.
Kwon, O.-S. (2007), "Probabilistic seismic assessment of structure, foundation, and soil interacting systems", Ph.D. Dissertation, University of Illinois, Urbana, IL, USA,
Kwon, O.-S. and Elnashai, A.S. (2006), "The effect of material and ground motion uncertainty on the seismic vulnerability curves of RC structure", Eng. Struct., 28, 289-303.
Lee, Y.-J., Song, J. and Tuegel, E.J. (2008), "Finite element system reliability analysis of a wing torque box", Proceedings of the 10th AIAA Nondeterministic Approaches Conference, Schaumburg, IL, April.
Liu, P.-L., Lin, H.-Z. and Der Kiureghian, A. (1989), CalREL User Manual. Report No. UCB/SEMM-89/18, University of California, Berkeley, CA, USA.
Melchers, R.E. (1999), Structural Reliability: Analysis and Prediction, (2nd edition), John Wiley & Sons, New York, NY, USA,
NIBS (1999), HAZUS, Earthquake Loss Estimation Technology, Technical Manual prepared by the National Institute of Buildings Sciences (NIBS) for the Federal Emergency Management Agency (FEMA).
Rackwitz, R. and Fiessler, B. (1978), "Structural reliability under combined load sequences", Comput. Struct., 9, 489-494.
Rossetto, T. and Elnashai, A.S. (2003), "Derivation of vulnerability functions for European-type RC structures based on observational data", Eng. Struct., 25(10), 1241-1263.
Song, J. (2007), Decision and Risk Analysis, Lecture notes, University of Illinois, Urbana, IL, USA, Feb. 28.
SwRI. (2011), NESSUS (ver 9.6), Southwest Research Institute, http://www.nessus.swri.org/ [cited 1 Mar. 2013].